Modeling peristaltic flow in vessels equipped with valves: implications for vasomotion in bat wing venules

A. Farina[a], L. Fusi[a,*], A. Fasano[a], A. Ceretani[b], F. Rosso[a]

[a] *Università degli Studi di Firenze, Dipartimento di Matematica e Informatica "U. Dini", Viale Morgagni 67/a, 50134, Firenze, Italy*
[b] *Universidad Austral, Dept. Matematica, Rosario, Argentina*

Abstract

We study the flow of a Newtonian fluid through a vessel provided with valves ensuring a unidirectional motion and whose walls are animated by periodic peristaltic waves. The ultimate target is to describe the phenomenon of vasomotion, consisting in periodic oscillations of blood vessels walls which is particularly important for the blood flow in veins. Here we formulate a mathematical model based on approximations of the flow equations due to the smallness of the radius-to-length ratio. In particular we examine venules equipped with just two valves, showing that the model reproduces the periodic pressure pulses that have been experimentally detected in venules of the bat wing. The flow generated by the synchronous vessel oscillations is recovered in the limit of large peristaltic wavelength.

Keywords: Vasomotion, Peristalsis, Newtonian fluid, Unilateral boundary conditions

1. Introduction

Blood vessels equipped with smooth muscle cells may undergo radial oscillations that are independent on heart pulsation or respiratory rhythm, and have indeed a different frequency. This phenomenon, called vasomotion, was first observed by T.W. Jones [18] in 1852 in the venules of the bat wing membrane. Its biological mechanisms have been studied in a number of papers. See the reviews [24], [13], [1] and the papers [22], [29], [21], [3], [14], [25], and

*Corresponding author: tel. +39552751437, Fax +39552751452
Email address: fusi@math.unifi.it (L. Fusi)

[20] proposing various mathematical models for the onset of persisting oscillations. Vasomotion frequency can (exceptionally) reach 25 cpm (0.42 Hz) and amplitude can peak to 100% of mean diameter [16]. More ordinary values are 10 cpm (0.17 Hz) and 25%. Since vasomotion is particularly active right where vessels resistance becomes large, it is a phenomenon considered with great attention, since it may have a critical influence on microcirculation.

In the recent paper [4] the authors, experimenting with bat wings, proved that venules vasomotion acts as a pump, increasing blood flow rate, thanks to the presence of backflow preventing valves. The experiments of [4] show that pressure exhibits large peaks during the vessel contraction. As we shall see, such a phenomenon can be explained assuming that the flow is regulated by just one inlet and one outlet valves.

In the present paper we formulate a mathematical model for an incompressible Newtonian flow in a cylindrical tube whose walls move exhibiting a periodic peristaltic wave, which in the long wavelength limit behaves like a synchronous oscillation. The tube has two valves: one at the entrance and the other at the outlet, having the task of making the flow unidirectional. An important assumption we are going to exploit is the smallness of the ratio

$$\varepsilon = \frac{R_o^*}{L^*} \ll 1, \tag{1}$$

where R_o^* is the maximum vessel radius and L^* is the vessel length (the symbol " * " denotes dimensional quantities). Following [4], we consider each valve as a compliant membrane which opens (respectively closes) when the pressure on its left side is larger (respectively smaller) than the one on its right side. The valve's action is thus modeled imposing a unilateral, or Signorini, boundary condition.

The analysis of the peristaltic flow, in a low Reynolds number and lubrication theory context, has been developed in a number of papers. Here we just mention [10], [26], [2], [30], devoted to the peristaltic wave optimal shape, and [27] in which the coupling between the flow and mechanics of the tube wall is studied. We also mention [15] in which a description of the blood vessel mechanics is developed. On the other hand, the literature treating peristaltic flow in vessels equipped with valves is not very large. We mention the pioneering paper [28] in which the flow in semi-infinite cylindrical vessel is analyzed. That paper focuses on the laminar flow driven by periodic wall contraction-expansion, but the condition imposed at the vessel end is just the one of no longitudinal motion, corresponding to the presence of seal

rather than a valve. Also the peristaltic flow in micro-devices equipped with valves has recently received attention in the context of the micro pumping technologies. In such a framework, the valves are devices of various nature whose purpose is to ensure unidirectional flow. We mention the interesting review [17], and [12] where a model for peristaltic micro-pumps with active valves has been developed. However the fluid mechanical setting considered in [12], as well as in many other papers devoted to micro pumping technologies, is totally different form the one we are going to model in this paper. Moreover, the models developed in those papers do not specifically enter the flow dynamics, being essentially oriented toward the determination of the overall output of the device.

The model we develop in this paper considers an incompressible Newtonian fluid (though more appropriate constitutive models [23] could be considered) and a contraction-expansion wave travelling along the vessel. In particular, denoting by λ^* the oscillation wavelength, we investigate two cases:

- $\lambda^* \gg L^*$, referred to as synchronous oscillation.
- $\lambda^* \approx L^*$, referred to as non synchronous oscillation.

We do not consider $\lambda^* \ll L^*$, since it is well known that in such a case peristalsis has basically no effect. The first case consists essentially in a uniform oscillation of the vessel walls, that, thanks to the inlet and outlet valves, contributes a net flow (which would not be the case in the absence of valves).

In the second case a wave profile travels along the vessel. Now, contrary to the first case, also in a valveless tube, we can have a non-zero average flow even if the external pressure gradient vanishes. The role of valves is to make the flow unidirectional, increasing the overall discharge.

The paper develops as follows: in § 2 we present the mathematical model. In particular, § 2.3 is devoted to a detailed discussion of the inlet and outlet boundary conditions. The synchronous oscillation model is illustrated in § 3, while the non synchronous oscillation in § 4. In § 5 we present some numerical simulations which, highlight physical consistency of the model. We indeed show that the first case (synchronous oscillation) is recovered from the second one in the limit of "long" wavelengths. Finally, in § 6 we show numerical solutions that fit reasonably well the experimentally detected pressure behavior in venules of bat wings [4].

2. Flow in a vessel equipped with an inlet and outlet valve

The physical effect of vasomotion on blood flow in venules equipped with valves preventing backflow is completely different from the one occurring in a valveless vessels. Indeed the valves confer to vasomotion a pumping action, whose contribution to the flow may be comparable to the one of the available pressure gradient.

While valves in the major veins had been observed since the early times of anatomy[1], the presence of valves in small veins has been underestimated or even ignored. The paper [5] reviews the historical perspective on the subject, particularly concerning microscopic valves, whose existence has been proved in venules as small as 25 μm diameter, in variable number (see [6], [7]).

With the target of fitting some of the experimental data of [4], we formulate a novel model for vessel equipped with just two valves placed at $x^* = 0$ and $x^* = L^*$, corresponding to vessel's inlet and outlet. The behavior of pressure shown in [4] cannot be explained without the presence of valves that act synchronously with the vessel oscillation. Indeed, a model with distributed valves, as the one developed in [8], cannot explain the pressure peaks detected in [4], since such a model encompasses a condition of pressure continuity which forces pressure to stay between the imposed inlet and outlet values.

2.1. The mathematical model

Let us now suppose that the vessel radius R^* evolves as a travelling wave with wavelength λ^*, i.e.

$$R^*\left(x^*, t^*\right) = R_o^* R\left(x^*, t^*\right), \qquad R\left(x^*, t^*\right) = 1 + \delta\Phi\left(\frac{x^*}{\lambda^*} - \frac{t^*}{T^*}\right), \quad (2)$$

where:

[1] There is some controversy about the discovery of vein valves. According to A. Caggiati the first to describe them was the Catalan Ludovicus Vassaeus in his *De Anatomen Corporis Humani tabulae quator* (Venice, 1542). See [6], [7], [5]. There were more or less contemporary or even earlier observations. In the old review paper [9] reference is made to unpublished findings on the subject by Giambattista Canano (1515-1579), professor of anatomy in Ferrara, that he reported to Vesalius in 1545. In the same year veins valves were described by the French anatomist Charles Estienne (1504-1564), who however claimed to have discovered them in 1538.

- $\Phi(\eta)$ is a periodic function (with period 1) such that $\max \Phi = 0$, $\min \Phi = -1$. We suppose also that Φ is decreasing in a fraction of the period (contraction phase) and increasing in the remaining fraction (expansion phase). In the physiological case of vasomotion the contraction fraction is typically < 0.5, [4].

- R_o^* is the maximum radius.

- $0 < \delta < 1$, is a dimensionless parameter, so that $R_o^* \delta$, gives the oscillation amplitude.

- λ^* is the wavelength and T^* is the wave period, which are linked to the wave velocity c^* by

$$c^* = \frac{\lambda^*}{T^*}. \tag{3}$$

We denote by $\boldsymbol{u}^*$ the tube surface velocity directed along the radius. From (2)

$$\boldsymbol{u}^* = \frac{\partial R^*}{\partial t^*} \boldsymbol{e}_r = -\dot{R}_{ref}^* \Phi' \left(\frac{x^*}{\lambda^*} - \frac{t^*}{T^*} \right) \boldsymbol{e}_r, \tag{4}$$

where $\Phi'(\eta) = d\Phi/d\eta$ and where

$$\dot{R}_{ref}^* = \frac{R_o^* \delta}{T^*}, \tag{5}$$

represents the average contraction velocity, so that we set $v_{2\ ref} = \dot{R}_{ref}^*$. In vasomotion $\dot{R}_{ref}^*$ is available from experiments. We introduce also $\lambda = \lambda^*/L^*$. As already stated in the introduction, we consider two cases:

1. λ^* much larger than L^* (more precisely $\lambda^{-1} \leq \varepsilon$), meaning that the vessel essentially undergoes spatially synchronous oscillations.
2. λ^* comparable with L^* i.e. $\lambda = \mathcal{O}(1)$.

In [11] we proved that when $\lambda^* \ll L^*$, peristalsis basically does not generate any flow. In dimensionless variables (2) becomes

$$R(x,t) = 1 + \delta \Phi \left(\frac{x}{\lambda} - t \right), \tag{6}$$

so that

$$\lambda \frac{\partial R}{\partial x} + \frac{\partial R}{\partial t} = 0.$$

The fluid can only enter the tube through the inlet surface

$$\{x^* = 0,\ 0 \le r^* \le R^*(0, t^*)\}$$

and flows out through the outlet surface

$$\{x^* = L^*,\ 0 \le r^* \le R^*(L^*, t^*)\}$$

.

We select the longitudinal reference velocity v^*_{ref} as follows

$$v^*_{ref} = \frac{1}{\varepsilon}\dot{R}^*_{ref} = \frac{1}{\varepsilon}\frac{R^*_o \delta}{T^*}. \tag{7}$$

So, if $\boldsymbol{v}^* = v^*_1\ \boldsymbol{e}_x + v^*_2\ \boldsymbol{e}_r$ is the fluid velocity, we set

$$v_1 = \frac{v^*_1}{v^*_{ref}}, \qquad v_2 = \frac{v^*_2}{\dot{R}^*_{ref}} = \frac{v^*_2}{\varepsilon v^*_{ref}},$$

entailing $\boldsymbol{v} = \ v_1 \boldsymbol{e}_x + \varepsilon v_2\ \boldsymbol{e}_r$. The reference pressure p^*_{ref} is defined as

$$\frac{p^*_{ref}}{L^*} = \frac{\mu^*}{{R^*_o}^2} v^*_{ref}\ .$$

The quantity p^*_{ref} represents the order of magnitude of the "effective pressure drop" caused by the oscillations of the vessel (inspired to Poiseuille's formula). The known imposed pressure difference is $\Delta p^* = p^*(0, t^*) - p^*(L^*, t^*) > 0$, and we consider

$$\Delta p = \frac{\Delta p^*}{p^*_{ref}} \le \mathcal{O}(1).$$

When $\Delta p \gg 1$, the flow is essentially dominated by the externally imposed pressure gradient and the effects due to the wall oscillations are hardly observable. We also introduce the dimensionless pressure

$$p = \frac{p^*(x^*, t^*) - p^*(L^*, t^*)}{p^*_{ref}}, \tag{8}$$

so that

$$p|_{inlet} = \Delta p, \qquad p|_{outlet} = 0. \tag{9}$$

We finally rescale the radial velocity of the vessel walls $\boldsymbol{u}^*$ by $\dot{R}^*_{ref}$, namely

$$\boldsymbol{u}^* = \dot{R}^*_{ref}\ u\ \boldsymbol{e}_r, \quad \text{with} \quad u = -\Phi'\left(\frac{x}{\lambda} - t\right) = -\frac{\lambda}{\delta}\frac{\partial R}{\partial x} = \frac{1}{\delta}\frac{\partial R}{\partial t}. \tag{10}$$

2.2. Flow equations

The fluid mechanical incompressibility yields

$$\frac{\partial v_1}{\partial x} + \frac{1}{r}\frac{\partial (r v_2)}{\partial r} = 0. \tag{11}$$

We assume that the Reynolds number characterizing the flow

$$\mathsf{Re} = \frac{\rho^* v^*_{ref} R^*_o}{\mu^*} \ ,$$

is negligible[2] so that the motion equation reduces to

$$-\nabla^* p^* + \mu^* \Delta^* \boldsymbol{v}^* = 0. \tag{12}$$

On the tube surface we set $\boldsymbol{v}^*|_{r^*=R^*} = \boldsymbol{u}^*$ so that, from (4)

$$v_1|_{r=R} = 0, \tag{13}$$

$$v_2|_{r=R} = -\Phi'\left(\frac{x}{\lambda} - t\right) = \frac{\partial \Phi}{\partial t} = -\frac{1}{\lambda}\frac{\partial \Phi}{\partial x}. \tag{14}$$

The line $r = 0$ is a symmetry axis so that

$$v_2|_{r=0} = 0, \quad \text{and} \quad \left.\frac{\partial v_1}{\partial r}\right|_{r=0} = 0. \tag{15}$$

Equations (12) become

$$-\frac{\partial p}{\partial x} + \varepsilon^2 \ \frac{\partial^2 v_1}{\partial x^2} + \frac{1}{r}\frac{\partial}{\partial r}\left(r\frac{\partial v_1}{\partial r}\right) = 0, \tag{16}$$

$$-\frac{1}{\varepsilon^2}\frac{\partial p}{\partial r} + \varepsilon^2 \ \frac{\partial^2 v_2}{\partial x^2} + \frac{1}{r}\frac{\partial}{\partial r}\left(r\frac{\partial v_2}{\partial r}\right) - \frac{v_2}{r^2} = 0, \tag{17}$$

which, at the leading order imply

$$p = p\,(x, t)\,,$$

and

$$-\frac{\partial p}{\partial x} + \frac{1}{r}\frac{\partial}{\partial r}\left(r\frac{\partial v_1}{\partial r}\right) = 0. \tag{18}$$

[2]Referring, for instance, to the data of [4] we have $\mathsf{Re} \approx 10^{-2}$.

Recalling boundary conditions (13) and $(15)_2$, we find

$$v_1(x,r,t) = -\frac{1}{4}\frac{\partial p}{\partial x}\left(R^2 - r^2\right), \tag{19}$$

(as expected) with $R(x,t)$ given by (6). We now insert (19) in (11), getting

$$4\frac{\partial}{\partial r}(r\,v_2) = \frac{\partial^2 p}{\partial x^2} r\left(R^2 - r^2\right) + 2r\frac{\partial p}{\partial x}R\frac{\partial R}{\partial x}.$$

Integrating between 0 and R and exploiting (14) we obtain

$$\frac{\partial}{\partial x}\left(\frac{R^4}{4}\frac{\partial p}{\partial x}\right) = 4Ru, \tag{20}$$

with u given by (10). So, taking the average on the vessel section, we have

$$\langle v_1\rangle = \frac{2}{R^2}\int_0^R \left(-\frac{1}{4}\frac{\partial p}{\partial x}\right)\left(R^2 - r^2\right) r\,dr = -\frac{1}{8}\frac{\partial p}{\partial x}R^2,$$

while the local discharge at time t (within an $\mathcal{O}(\varepsilon)$ approximation) is

$$Q(x,t) = \pi R^2 \langle v_1\rangle = -\pi\frac{R^4}{8}\frac{\partial p}{\partial x}. \tag{21}$$

2.3. Boundary conditions at the vessel ends

The valves are placed at the vessels ends, and act to prevent backflow. The valves dynamics is indeed simple: the inlet valve closes when pressure exceeds the inlet one; the outlet valve closes when pressure falls below the outlet one. In other words, at $x = 0$, inlet valve, two conditions have to be fulfilled

$$Q(0,t) \geq 0, \quad \Leftrightarrow \quad \left.\frac{\partial p}{\partial x}\right|_{x=0} \leq 0, \tag{22}$$

$$p(0,t) \geq \Delta p. \tag{23}$$

The first condition simply states that backflow cannot occur, while the second one guarantees that $p(0,t)$ can never drop below the externally imposed

pressure. Moreover, it is necessary that at least one of such condition holds as an equality. Hence the inlet boundary conditions summarize as follows

$$\begin{cases} \left.\dfrac{\partial p}{\partial x}\right|_{x=0} (p(0,t) - \Delta p) = 0 \\ \\ \left.\dfrac{\partial p}{\partial x}\right|_{x=0} \leq 0, \\ \\ p(0,t) \geq \Delta p. \end{cases} \tag{24}$$

This is a typical unilateral boundary condition - also known as Signorini type condition - which is frequently encountered in continuum mechanics (see, for instance, [19]). Similarly, the boundary conditions at $x = 1$ are

$$\begin{cases} \left.\dfrac{\partial p}{\partial x}\right|_{x=1} p(1,t) = 0, \\ \\ \left.\dfrac{\partial p}{\partial x}\right|_{x=1} \leq 0, \\ \\ p(1,t) \leq 0. \end{cases} \tag{25}$$

In the sequel we calculate only the pressure profile, since the expressions of velocity and discharge can then be obtained easily.

3. First case: $\boldsymbol{\lambda^{-1} \leq \varepsilon}$, synchronous oscillation

This case, as stated more than once, corresponds to a spatially uniform contraction/expansion of the vessel. Therefore $R = R(t)$ and, because of (10),

$$u = \frac{1}{\delta} \dot{R}(t).$$

Formula (20) can be rewritten as

$$\frac{\partial^2 p}{\partial x^2} = \frac{16}{\delta} \frac{\dot{R}}{R^3}, \quad \Rightarrow \quad \begin{cases} p(x,t) = \dfrac{8}{\delta} \dfrac{\dot{R}(t)}{R^3(t)} x^2 + A(t)\, x + B(t), \\ \\ \dfrac{\partial p(x,t)}{\partial x} = \dfrac{16}{\delta} \dfrac{\dot{R}(t)}{R^3(t)} x + A(t), \end{cases}$$

where $A(t)$, $B(t)$ have to be determined. Interestingly

$$\frac{\dot{R}}{R^3} = -\frac{\pi}{2}\frac{d}{dt}\left(\frac{1}{S(t)}\right),$$

where $S(t) = \pi R^2(t)$ is the vessel cross section area. Condition (24) rewrites as

$$\begin{cases} A(t)\left(B(t) - \Delta p\right) = 0, \\ A(t) \leq 0, \\ B(t) - \Delta p \geq 0, \end{cases} \tag{26}$$

while (25) takes the form

$$\begin{cases} \left(\dfrac{8}{\delta}\dfrac{\dot{R}(t)}{R^3(t)} + A(t) + B(t)\right)\left(\dfrac{16}{\delta}\dfrac{\dot{R}(t)}{R^3(t)} + A(t)\right) = 0, \\ \dfrac{16}{\delta}\dfrac{\dot{R}(t)}{R^3(t)} + A(t) \leq 0, \\ \dfrac{8}{\delta}\dfrac{\dot{R}(t)}{R^3(t)} + A(t) + B(t) \leq 0. \end{cases} \tag{27}$$

Let us consider the compression phase $\dot{R} < 0$, and assume first $A = 0$ (entrance valve engaged). From $(27)_1$

$$B(t) = \frac{8}{\delta}\frac{\left|\dot{R}\right|}{R^3},$$

meaning $p(1,t) = 0$. Of course condition $(26)_3$ has to be satisfied so that

$$\frac{8}{\delta}\frac{\left|\dot{R}\right|}{R^3} \geq \Delta p. \tag{28}$$

On the other hand if

$$\frac{8}{\delta}\frac{\left|\dot{R}\right|}{R^3} < \Delta p, \tag{29}$$

the entrance valve is open and the solution is

$$B(t) = \Delta p \quad \text{and} \quad A(t) = -\left(\frac{8}{\delta}\frac{\dot{R}(t)}{R^3(t)} + \Delta p\right).$$

Hence, during the compression phase we have

$$p(x,t) = \begin{cases} \dfrac{8}{\delta}\dfrac{\dot{R}}{R^3}\left(x^2-1\right), & \text{if} \quad \dfrac{8}{\delta}\dfrac{\left|\dot{R}\right|}{R^3} \geq \Delta p, \\ \\ \dfrac{8}{\delta}\dfrac{\dot{R}}{R^3}\left(x^2-x\right) - \Delta p\left(x-1\right), & \text{if} \quad \dfrac{8}{\delta}\dfrac{\left|\dot{R}\right|}{R^3} < \Delta p, \end{cases} \tag{30}$$

corresponding to a closed or open entrance valve. In the expansion phase $\dot{R} > 0$, we first consider

$$A = -\frac{16}{\delta}\frac{\dot{R}}{R^3},$$

i.e. the exit valve is closed, respectively. We conclude that B equals the inlet dimensionless pressure $B(t) = \Delta p$ and, recalling $(27)_3$, we observe that the compatibility condition (28) must once again be fulfilled. On the other hand, when condition (29) holds the exit valve is open and the condition $p(1,t) = 0$ yields

$$A(t) = -\left(\frac{8}{\delta}\frac{\dot{R}(t)}{R^3(t)} + \Delta p\right) \quad \text{and} \quad B(t) = \Delta p.$$

Summarizing, during the expansion phase the pressure is

$$p(x,t) = \begin{cases} \Delta p + \dfrac{8}{\delta}\dfrac{\dot{R}}{R^3}\left(x^2-2x\right), & \text{if} \quad \dfrac{8}{\delta}\dfrac{\dot{R}}{R^3} \geq \Delta p, \\ \\ \dfrac{8}{\delta}\dfrac{\dot{R}}{R^3}\left(x^2-x\right) - \Delta p\left(x-1\right), & \text{if} \quad \dfrac{8}{\delta}\dfrac{\dot{R}}{R^3} < \Delta p, \end{cases} \tag{31}$$

corresponding to a closed or open exit valve, respectively. We remark that when $\dot{R} \equiv 0$, equations (30)-(31) provide the classical linear profile

$$p(x,t) = \Delta p\ (1-x).$$

We also observe that when a valve at one end is closed the one at the opposite end is open, so that the flux has no interruption.

4. Second case: $\boldsymbol{\lambda = \mathcal{O}(1)}$, non-synchronous oscillation

Recalling (20) and (10), we write

$$\frac{\partial}{\partial x}\left(\frac{R^4}{8}\frac{\partial p}{\partial x}\right) = -\frac{\lambda}{\delta}\frac{\partial R^2}{\partial x}. \tag{32}$$

Integrating once we get

$$\frac{\partial p}{\partial x} = -\frac{8\lambda}{\delta}\frac{1}{R^2} + \frac{\mathcal{A}(t)}{R^4}, \tag{33}$$

where $\mathcal{A}(t)$ is unknown at this stage. Integrating once more

$$p(x,t) \ = \mathcal{B}(t) - \frac{8\lambda}{\delta}\int_0^x \frac{dx'}{R^2} + \mathcal{A}(t)\int_0^x \frac{dx'}{R^4},$$

where $\mathcal{B}(t)$ is unknown as well.

Remark 1. *Exploiting (21), formula (32) can be rewritten as*

$$\frac{\partial Q(x,t)}{\partial x} = \frac{\pi\lambda}{\delta}\frac{\partial R^2}{\partial x}, \quad \Rightarrow \quad Q(x,t) = \frac{\pi\lambda}{\delta}R^2(x,t) + F(t).$$

The latter allows to evaluate the mean difference between the inlet discharge (i.e. at $x = 0$) and the outlet discharge (at $x = 1$), namely

$$\langle \Delta Q(t) \rangle = \int_0^1 [Q(0,t) - Q(1,t)]dt.$$

We have

$$\langle \Delta Q(t) \rangle = \frac{\pi\lambda}{\delta}\left(\int_0^1 R^2(0,t)dt - \int_0^1 R^2(1,t)dt\right) = 0,$$

compatibly with the fluid incompressibility.

We introduce

$$R_{in}(t) = R(0,t), \quad R_{out}(t) = R(1,t),$$

$$S_{in}(t) = \pi R_{in}^2(t), \quad S_{out}(t) = \pi R_{out}^2(t),$$

and, proceeding as in § 3, we consider two cases:

$$(a) \qquad S_{in}(t) < S_{out}(t) \quad \Leftrightarrow \quad R_{in}(t) < R_{out}(t)$$

$$(b) \qquad S_{in}(t) \geq S_{out}(t) \quad \Leftrightarrow \quad R_{in}(t) \geq R_{out}(t)$$

We define

$$\mathcal{I}_2(t) = \int_0^1 \frac{dx}{R^2(x,t)}, \qquad \mathcal{I}_4(t) = \int_0^1 \frac{dx}{R^4(x,t)}.$$

In case (a) the boundary conditions (24), (25) yields

$$\mathcal{A}(t) = \frac{8\lambda}{\delta} R_{in}^2(t),$$

and

$$\mathcal{B}(t) = \frac{8\lambda}{\delta}\left[\mathcal{I}_2(t) - R_{in}^2(t)\,\mathcal{I}_4(t)\right],$$

provided

$$\frac{8\lambda}{\delta}\left[\mathcal{I}_2(t) - R_{in}^2(t)\,\mathcal{I}_4(t)\right] \geq \Delta p\ .$$

On the other hand, when

$$\Delta p > \frac{8\lambda}{\delta}\left[\mathcal{I}_2(t) - R_{in}^2(t)\,\mathcal{I}_4(t)\right], \tag{34}$$

we take

$$\mathcal{B}(t) = \Delta p,$$

and

$$\mathcal{A}(t) = \frac{\frac{8\lambda}{\delta}\mathcal{I}_2(t) - \Delta p}{\mathcal{I}_4(t)}, \tag{35}$$

Since conditions $(24)_3$ and $(25)_3$ are fulfilled, we need to prove only $(24)_2$ from which $(25)_2$ automatically follows because $R_{in}^2 < R_{out}^2$. Rewriting $(24)_2$ as

$$\mathcal{A} \leq \frac{8\lambda}{\delta} R_{in}^2$$

and using (35), we immediately obtain (34). Concerning case (b), we have

$$\mathcal{B} = \Delta p,$$

and

$$\mathcal{A}(t) = \frac{8\lambda}{\delta} R_{out}^2(t), \quad \text{if} \quad \Delta p \leq \frac{8\lambda}{\delta} \left[\mathcal{I}_2(t) - R_{out}^2(t)\, \mathcal{I}_4(t)\right],$$

or $\mathcal{A}$ given by (35) in case $\Delta p > \frac{8\lambda}{\delta} \left[\mathcal{I}_2(t) - R_{out}^2(t)\, \mathcal{I}_4(t)\right]$. We have thus proved the following

- If $S_{in} < S_{out}$, and $\Delta p \leq \frac{8\lambda}{\delta} \left[\mathcal{I}_2(t) - R_{in}^2(t)\, \mathcal{I}_4(t)\right]$ then

$$p(x,t) = \frac{8\lambda}{\delta} \int_x^1 \left(\frac{1}{R^2(x',t)} - \frac{R_{in}^2(t)}{R^4(x',t)} \right) dx'. \tag{36}$$

- If $S_{in} < S_{out}$, and $\Delta p > \frac{8\lambda}{\delta} \left[\mathcal{I}_2(t) - R_{in}^2(t)\, \mathcal{I}_4(t)\right]$ then

$$p(x,t) = \Delta p \left(1 - \frac{1}{\mathcal{I}_4(t)} \int_0^x \frac{dx'}{R^4} \right) + \frac{8\lambda}{\delta} \int_0^x \left(\frac{1}{R^4} \frac{\mathcal{I}_2(t)}{\mathcal{I}_4(t)} - \frac{1}{R^2} \right) dx'. \tag{37}$$

- If $S_{in} \geq S_{out}$, and $\Delta p \leq \frac{8\lambda}{\delta} \left[\mathcal{I}_2(t) - R_{out}^2(t)\, \mathcal{I}_4(t)\right]$ then

$$p(x,t) = \Delta p + \frac{8\lambda}{\delta} \int_0^x \left(\frac{R_{out}^2}{R^4} - \frac{1}{R^2} \right) dx'. \tag{38}$$

- If $S_{in} \geq S_{out}$, and $\Delta p > \frac{8\lambda}{\delta} \left[\mathcal{I}_2(t) - R_{out}^2(t)\, \mathcal{I}_4(t)\right]$ then

$$p(x,t) = \Delta p \left(1 - \frac{1}{\mathcal{I}_4(t)} \int_0^x \frac{dx'}{R^4} \right) + \frac{8\lambda}{\delta} \int_0^x \left(\frac{1}{R^4} \frac{\mathcal{I}_2(t)}{\mathcal{I}_4(t)} - \frac{1}{R^2} \right) dx'. \tag{39}$$

5. Numerical simulations: synchronous and non synchronous oscillations

In this section we provide some numerical simulations. We begin by showing the behavior of the pressure selecting the function $\Phi(\eta)$ defined in (2) in the following way

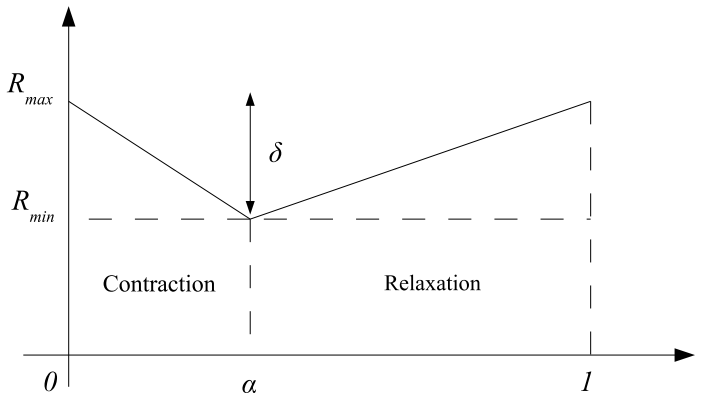

Figure 1: The function $R(\eta)$.

$$\Phi(\eta) = \begin{cases} -\dfrac{\eta}{\alpha}, & \eta \in [0, \alpha], \\ \\ -1 + \dfrac{(\eta - \alpha)}{(1 - \alpha)}, & \eta \in [\alpha, 1]. \end{cases}$$

This selection implies that the oscillation is formed by a contraction ($\alpha-$fraction of the period) and an expansion ($(1-\alpha)-$fraction of the period). The function $R(\eta)$ (Fig. 1) is thus

$$R(\eta) = \begin{cases} 1 - \dfrac{\delta\eta}{\alpha}, & \eta \in [0, \alpha], \\ \\ (1 - \delta) + \dfrac{\delta(\eta - \alpha)}{(1 - \alpha)}, & \eta \in [\alpha, 1]. \end{cases} \tag{40}$$

The choice of R is purely illustrative: other choices are clearly possible. In Fig.s 2, 3 we plot the pressure profile $p(x,t)$ for different values of λ using the expressions (36)-(39) derived in § 4. In particular, we plot p as a function

of x for $t \in [0,1]$. The inlet pressure Δp is taken equal to one. As one can see, when λ approaches $O(10^3)$, the pressure plots stabilize, so that a further increase of λ does not produce any change in the pressure profiles. This fact can be explained observing that for λ sufficiently large the oscillation is essentially synchronous (i.e. spatially uniform).

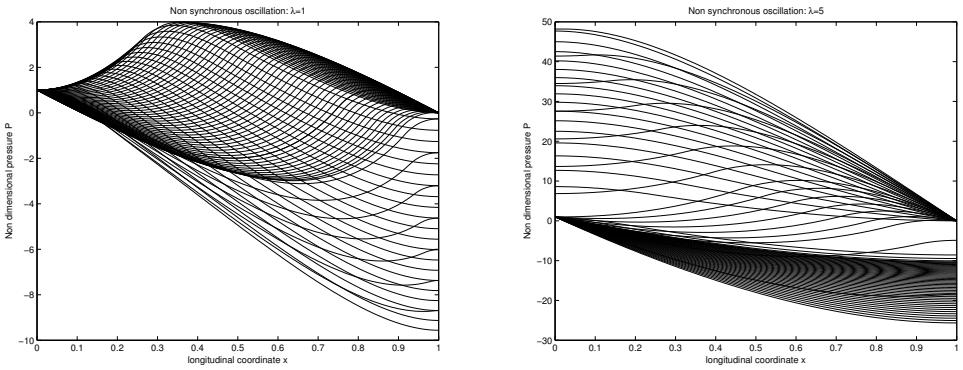

$\lambda = 1$ $\qquad\qquad$ $\lambda = 5$

Figure 2: Dimensionless pressure profiles $p(x,t)$ for different values of λ, obtained using formulas (36)-(39).

We remark that the model is physically consistent, since the plot corresponding to the synchronous oscillation essentially coincides with the plot corresponding to the non synchronous oscillation with $\lambda \gg 1$ (see Fig. 4).

6. Comparison with experimental data

In order to compare our model with the experimental data provided in [4] we consider $R(t)$ that reproduces the synchronous radius oscillats of a representative venule, as shown in Fig. 3 of [4], on the basis of experimental measures. In particular, we select a non dimensional $R(t)$ of the type[3]

$$R(t) = at^3(1-t^3)^3 + (1-\delta). \tag{41}$$

and we use the parameter a to fit the experimental R^*. From Fig. 3 of [4] we notice that $R_o^* \approx 70\ \mu m$, $T^* \approx 6\ sec$, $\delta = 0.25$, so that we can easily

[3]Recall that δ denotes the oscillation amplitude.

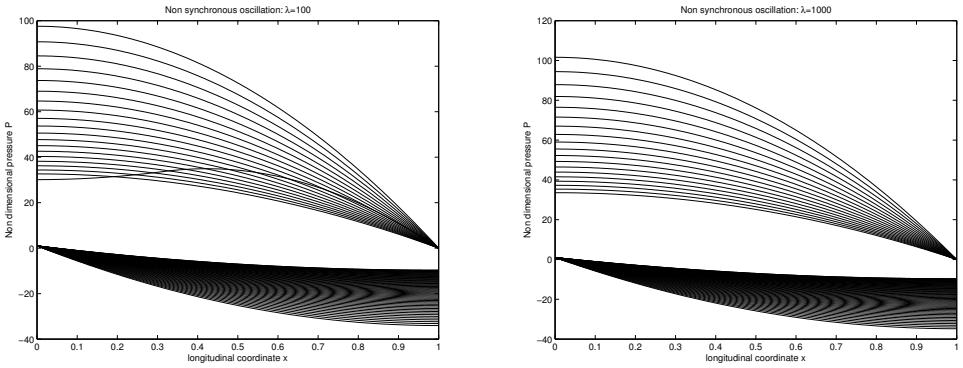

$\lambda = 100$ $\lambda = 1000$

Figure 3: Dimensionless pressure profiles $p(x,t)$ for different values of λ, obtained using formulas (36)-(39).

find the fitting parameter a, which turns out to be $a \approx 2.37$. In Fig. 5 we show the plot of the non dimensional radius oscillation given by (41) and the experimental data.

Then we use the synchronous model (30), (31) defined in Section 3 to plot the non dimensional pressure close to the inlet $x = 0$. The characteristic values extrapolated from [4] are

$$\dot{R}^*_{ref} = 3.04\ \frac{\mu m}{sec}, \qquad v^*_{ref} = 1.22\ \frac{mm}{sec}$$

$$p^*_{ref} = 0.37\ cmH_2O, \qquad \varepsilon = 2.5 \times 10^{-3}.$$

In Fig. 6 we show the comparison between the experimental data of [4] (Fig. 5, luminal pressure) and the pressure profile predicted by the model. As one can see, the agreement is quite satisfactory, considering the simplicity of the model, which includes just two valves (neglecting their inertia) and operates in a Newtonian context. Numerical simulations of non-synchronous oscillations (peristaltic motion with wavelength comparable to the vessel length, not shown here) did not provide a good fit. Therefore the synchronous two-valve model seems adequate to simulate the phenomenon of vasomotion in the bat wing venules.

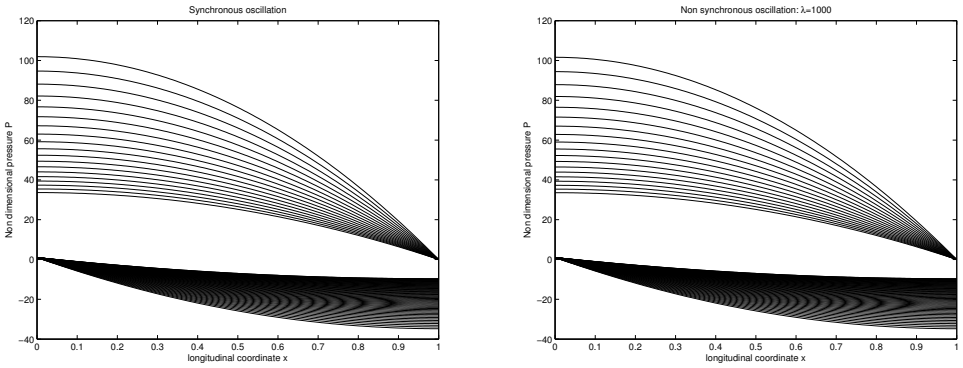

Synchronous oscillation Non Synchronous oscillation, $\lambda = 1000$

Figure 4: Comparison between the synchronous and non synchronous case for $\lambda = 1000$.

7. Conclusions

We have formulated a mathematical model for incompressible Newtonian flows in tubes subject to peristaltic motion and equipped with an inlet and an outlet valve, ensuring one directional motion. The biological application we have in mind is the phenomenon of vasomotion particularly important for small vessels (venules). The model starts from the basic laws of fluid dynamics and, exploiting the smallness of the radius/length ratio, derives simpler approximating equations which are nevertheless rather accurate.

The case of synchronous oscillations, which is typical of venules, can be seen as the limit of the peristaltic motion when the wavelength is much larger than the vessel length. Such a feature has been confirmed on the basis of numerical computation. It seems reasonable that an excitation wave propagates along the vessel at a sufficiently high speed to eventually look synchronous. It is nevertheless interesting to consider the more general case of peristaltic propulsion, since it applies to larger veins. We have compared our simulations with the experimental results of [4] on the bat wing venules, characterized by periodic pressure pulses. We have obtained an agreement which is remarkable, considering the simplicity of the model core. Thus the present model indicates that, at least for the biological case of [4], the scheme with two valves provides a quite reasonable description of the phenomenon.

[1] Aalkjaer C., Nilsson H., Vasomotion: cellular background for the oscil-

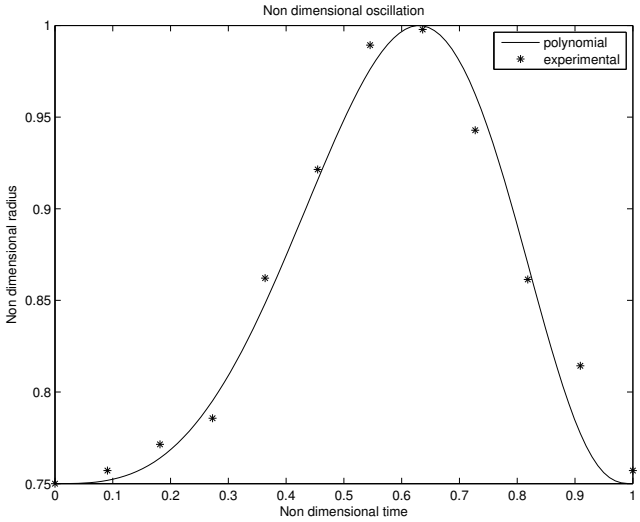

Figure 5: Radius oscillation: interpolation of the experimental data of [4].

lator and for the synchronization of smooth muscle cells. *British Journal of Pharmacology* **144**, 2005, 605–616.

[2] Brown T. D., Hung T.K., Computational and experimental investigations of two-dimensional nonlinear peristaltic flows. *J. Fluid Mech.* **83**, 1977, 249-272.

[3] de Wit C., Closing the gap at hot spots, Circ Res, **100**, 2007, 931-933.

[4] Dongaonkar R. M., Quick C. M., Vo J. C., Meisner J. K., Laine G. A., Davis M. J., Stewart, R. H., Blood flow augmentation by intrinsic venular contraction in vivo. *Am. J. Physiol. Regul. Integr. Comp. Physiol.*, **302**, 2012, R1436–R1442.

[5] Caggiati A., Phillips M., Lametschwandtner A., Allegra C, Valves in small veins and venules. *Eur. J. Vasc. Endovasc. Surg.* **32**, 2006, 447-452.

[6] Caggiati A., Bertocchi, P., Regarding "Fact and fiction surrounding the discovery of the venous valves". *Journal of Vascular Surgery* **33**, 2001, 1317.

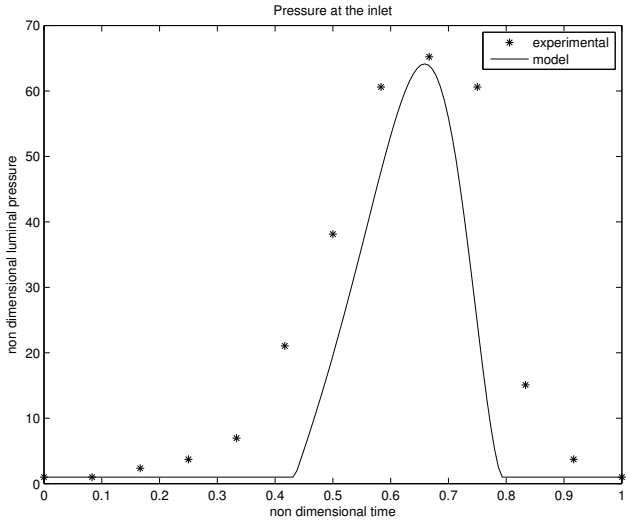

Figure 6: Comparison with experimental data of [4].

[7] Caggiati A., The venous valves in the lower limbs, *Phlebolymphology* **20**, 2013, 87-95.

[8] Farina A., Fasano A., Incompressible flows through slender oscillating vessels provided with distributed valves. Accepted for pubblication on *Adv. Math. Sci. Appl.* 2015.

[9] Franklin K. J., Valves in veins: an historical survey, *Proc. Royal Soc. Med. Section of the History of medicine,* 1927, 1-33.

[10] Fung Y. C., Yih C. S., Peristaltic transport. *J. Appl. Mech.* **35**, 1968, 669–675.

[11] Fusi L., Farina A., Fasano A., Short and long wave peristaltic flow: modeling and mathematical analysis. *International Journal of Applied Mechanics* **7**, 2015, DOI: 10.1142/S1758825115400141.

[12] Goldschmidtboing F., Doll A., Heinrichs M., Woias P., Schrag H. J., Hopt U. T., A generic analytical model for micro-diaphragm pumps with active valves. *J. Micromech. Microeng.* **15,** 2005, 673–683.

[13] Haddock R.E., Hill C.E., Rhythmicity in arterial smooth muscle. *J. Physiol.* **56**, 2005, 645–656.

[14] Haddock R. E., Hirst G. D. S., Hill C. E., Voltage independence of vasomotion in isolated irideal arterioles of the rat. *Journal of Physiology* **540**, 2002, 219–229.

[15] Horgan C. O., Saccomandi G., A description of arterial wall mechanics using limiting chain extensibility constitutive models, *Biomechan. Model Mechanobiol.,* **1**, 2003, 251 – 266

[16] Intaglietta M., Vasomotion and flowmotion: physiological mechanisms and clinical evidence. *Vascular Medicine Review* **1**, 1990, 1101-112.

[17] Iverson B. D., Garimella S. V., Recent advances in microscale pumping technologies: a review and evaluation. *Microfluid Nanofluid.* **5**, 2008, 145–174, DOI: 10.1007/s10404-008-0266-8.

[18] Jones T. W., Discovery that veins of the bat's wing (which are furnished with valves) are endowed with rhythmical contractility and that the onward flow of blood is accelerated by each contractio. *Philos. Trans. R. Soc. Lond.* **142**, 1852, 131–136.

[19] Kikuchi N., Oden J. T., Contact problem in elasticity: a study of variational inequalities and finite element methods, In *SIAM Study in Applied Mathematics*, Vol. 8, 1988.

[20] Koenigsberger M., Sauser R., Beny, J. L., Meister J. J., Effects of arterial wall stress on vasomotion. *Biophysical Journal* **91**, 2006, 1663–1674.

[21] Matchkov V. V., Gustafsson H., Rahman A., Boedtkjer D. M., Gorintin S., Hansen A. K., Bouzinova E. V., Praetoriu H. A., Aalkjaer C., Nilsson H., Interaction between Na/K pump and Na/Ca2 exchanger modulates intercellular communication. *Circ Res.* **100**, 2007, 1026–1035.

[22] Parthimos D., Haddock R. E., Hill C. E., Griffith T. M., Dynamics of a three-variable nonlinear model of vasomotion: Comparison of theory and experiment. *Biophysical Journal* **93**, 2007, 1534–1556.

[23] Anand M., Rajagopal K.R., A shear-thinning viscoelastic fluid model for describing the floe of blood, *Int. J. Cardiovascular Medicine Science*, **4**, 2004, 59–68.

[24] Reho J. J., Zheng X., Fisher S. A., Smooth muscle contractile diversity in the control of regional circulations. *Am. J. Physiol. Heart Circ. Physiol.* **306**, 2014, H163–H172.

[25] Rivadulla C., de Labra C., Grieve K. L., Cudeiro J., Vasomotion and neurovascular coupling in the visual thalamus in vivo. *PLOS ONE.* **6**, 2011, 28746.

[26] Shapiro A. H., Jaffrin M. Y., Weinberg S. L., Peristaltic pumping with long wavelengths at low Reynolds number. *J. Fluid Mech.* **37**, 1969, 799–825.

[27] Takagi D., Balmforth N. J., Peristaltic pumping of viscous fluid in an elastic tube. *J. Fluid Mech.* **672**, 2011, 196–218.

[28] Uchida S., Aok H., Unsteady flows in a semi-infinite contracting or expanding pipe. *J. Fluid Mech.* **82**, 1977, 371- 387.

[29] Ursino M., Fabbri G., Belardinelli E., A mathematical analysis of vasomotion in the peripheral vascular bed. *Cardioscience* **3**, 1992, 13-25.

[30] Walker S. W., Shelley M. J., Shape optimization of peristaltic pumping. *J. Comput. Phys.* **229**, 2010, 1260–1291.